

Article

Self-Humidifying Membrane for High-Performance Fuel Cells Operating at Harsh Conditions: Heterojunction of Proton and Anion Exchange Membranes Composed of Acceptor-Doped SnP_2O_7 Composites

Pilwon Heo ¹, Mijeong Kim ², Hansol Ko ², Sang Yong Nam ²  and Kihyun Kim ^{2,*}

¹ Fuel Cell Engineering Team, Hyundai Mobis, 37, Cheoldobangmulgwan-ro, Uiwang-si 16082, Korea; pilwon@mobis.co.kr

² Department of Materials Engineering and Convergence Technology, Gyeongsang National University, Jinju 52828, Korea; mijeong@gnu.ac.kr (M.K.); hansol.pmc@gnu.ac.kr (H.K.); walden@gnu.ac.kr (S.Y.N.)

* Correspondence: kihyun@gnu.ac.kr; Tel.: +82-055-772-1655

Abstract: Here we suggest a simple and novel method for the preparation of a high-performance self-humidifying fuel cell membrane operating at high temperature (>100 °C) and low humidity conditions (<30% RH). A self-humidifying membrane was effectively prepared by laminating together proton and anion exchange membranes composed of acceptor-doped SnP_2O_7 composites, $\text{Sn}_{0.9}\text{In}_{0.1}\text{H}_{0.1}\text{P}_2\text{O}_7/\text{Sn}_{0.92}\text{Sb}_{0.08}(\text{OH})_{0.08}\text{P}_2\text{O}_7$. At the operating temperature of 100 °C, the electrochemical performances of the membrane electrode assembly (MEA) with this heterojunction membrane at 3.5% RH were better than or comparable to those of each MEA with only the proton or anion exchange membranes at 50% RH or higher.

Keywords: self-humidifying membrane; acceptor doped SnP_2O_7 ; heterojunction membrane; proton exchange membrane; anion exchange membrane



Citation: Heo, P.; Kim, M.; Ko, H.; Nam, S.Y.; Kim, K. Self-Humidifying Membrane for High-Performance Fuel Cells Operating at Harsh Conditions: Heterojunction of Proton and Anion Exchange Membranes Composed of Acceptor-Doped SnP_2O_7 Composites. *Membranes* **2021**, *11*, 776. <https://doi.org/10.3390/membranes11100776>

Academic Editor: Fatemeh Razmjooei

Received: 3 September 2021

Accepted: 5 October 2021

Published: 11 October 2021

Publisher's Note: MDPI stays neutral with regard to jurisdictional claims in published maps and institutional affiliations.



Copyright: © 2021 by the authors. Licensee MDPI, Basel, Switzerland. This article is an open access article distributed under the terms and conditions of the Creative Commons Attribution (CC BY) license (<https://creativecommons.org/licenses/by/4.0/>).

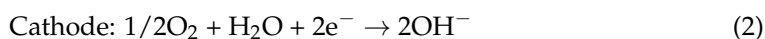
1. Introduction

Polymer electrolyte membrane fuel cells (PEMFCs) have been intensively studied with the goal of commercialization [1–3]. An important issue that has recently emerged for the wide application of PEMFCs is to increase the operating temperature up to 120 °C while simultaneously decreasing the relative humidity (RH) below 30%, as suggested by the U.S. Department of Energy (DOE) [4,5]. However, commercially available perfluorosulfonic acid membranes (PFSAs), such as Nafion (Dupont Chemical, Wilginton, DE, USA) and Aciplex (Asahi Chemical Inc., Osaka, Japan), cannot function as polymer electrolyte membranes under such harsh operating conditions because the absorbed water molecules facilitating the ion transportation are evaporated, leading to a significant decrease in the membrane conductivity [6]. To date, several promising membranes based on hydrocarbon polymers have been reported, such as polyether ether ketone (PEEK) [7], poly(arylene ether sulfone) (PAES) [8,9], polysulfone (PSf) [10], and polybenzimidazole (PBI) [11,12]. Among these membranes, the H_3PO_4 -doped PBI membrane exhibits conductivities of ca. $10^{-2} \text{ S cm}^{-1}$ above 100 °C and low RH condition. However, the use of a membrane electrode assembly employing the H_3PO_4 -doped PBI membrane is problematic since some of the H_3PO_4 permeates into the cathode and poisons the Pt catalyst by the strong adsorption of phosphate anions [13].

As part of an alternative approach to the development of electrolyte membranes operating at high temperature and low RH condition, various composite membranes with self-humidification ability that can be prepared by simple methods have been proposed. Self-humidifying membranes are typically divided into three main types according to the materials incorporated in the membrane system: (1) Pt or Pt/C catalysts promote

the reaction of hydrogen and oxygen from the anode and the cathode, respectively, to produce water in the membrane [14]; (2) hygroscopic metal oxides, such as SiO₂ and TiO₂, bound water molecules and maintain the hydration of the membrane [14,15]; and (3) proton-conductive materials, such as zirconium phosphate and heteropolyacids [16,17], improve the proton conducting behavior of the membrane at high temperature and low RH condition. However, although these types of membranes are useful for the harsh operating conditions of PEMFCs, they have some problems that remain unsolved: (1) the heterogeneous dispersion of Pt may lead to local electronic conduction throughout the membrane [18]; (2) the increase of the additive contents may lead to increase the ohmic resistance of the membrane [19]; (3) the poor compatibility between the additive and membrane may decrease the mechanical properties of the membrane [20].

These issues examine the heterojunction of proton and anion exchange membranes as a novel method for the development of self-humidifying membranes. When the two laminated membranes are arranged by placing the proton and anion exchange membranes at the anode and cathode sides, respectively, the following electrode reactions occur during cell discharge:



At the interface between the two membranes, it is proposed that the following reaction occurs, as shown in Figure 1a:



The resulting water product humidifies the two membranes, which improves their ionic conductivities at high temperature and low RH condition. The three problems noted above can essentially be avoided by using this technology, because it does not utilize any additives. An additional benefit of this method is the lower fabrication cost of the self-humidifying membrane, as the two membranes are simply pressed together.

In this work, acceptor-doped SnP₂O₇ is used as proton and anion exchange membranes because these compounds have high proton or hydroxide ion conductivity (>10⁻² S cm⁻¹) under the temperature range from 50 to 300 °C [21]. The SnP₂O₇ structures are characterized by the presence of intersecting zigzag tunnels delimited by pentagonal windows, which provide many ion exchangeable sites and conducting pathways [22]. The ion-exchange capabilities are incorporated into the bulk SnP₂O₇ through the partial substitution of Sn⁴⁺ cations with low valency In³⁺ and high valency Sb⁵⁺ due to the charge compensation of the dopant cations [18,19]. The optimal compositions of these acceptor-doped SnP₂O₇ compounds were determined to be Sn_{0.9}In_{0.1}H_{0.1}P₂O₇ and Sn_{0.92}Sb_{0.08}(OH)_{0.08}P₂O₇. Their crystalline structures are illustrated in Figure 1b. The self-humidification of the membrane during the fuel cell operation is demonstrated by electrical conductivity and water uptake measurements. Further, the self-humidification effect on the IR loss of the membrane during the operation is quantified through electrochemical measurements.

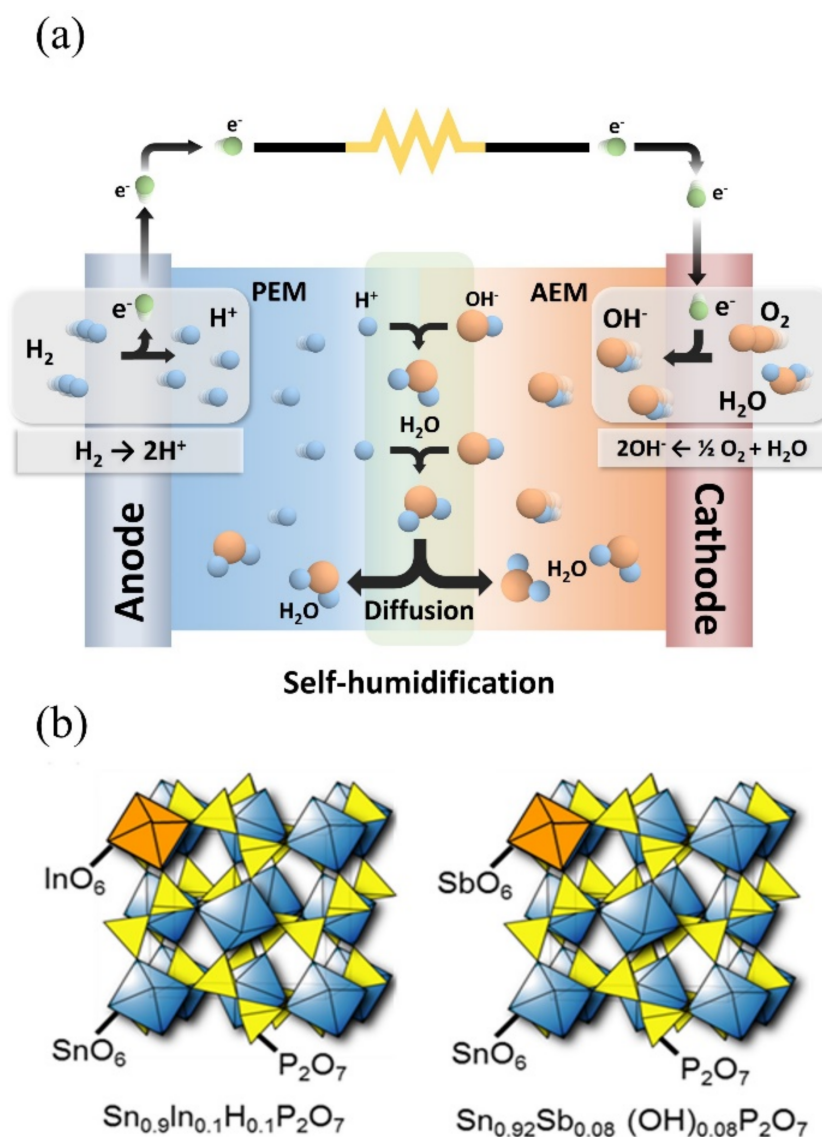


Figure 1. (a) schematic diagram of self-humidifying heterojunction membrane fuel cell and (b) crystalline structure of $\text{Sn}_{0.9}\text{In}_{0.1}\text{H}_{0.1}\text{P}_2\text{O}_7$ and $\text{Sn}_{0.92}\text{Sb}_{0.08}(\text{OH})_{0.08}\text{P}_2\text{O}_7$.

2. Experimental

2.1. Sample Preparation

The $\text{Sn}_{0.9}\text{In}_{0.1}\text{H}_{0.1}\text{P}_2\text{O}_7$ and $\text{Sn}_{0.92}\text{Sb}_{0.08}(\text{OH})_{0.08}\text{P}_2\text{O}_7$ membranes were prepared by following the previously reported procedures [20,23]: briefly, SnO_2 and In_2O_3 or Sb_2O_5 were mixed with a H_3PO_4 solution at a molar ratio of $\text{P}/(\text{Sn} + \text{In} \text{ or } + \text{Sb}) = 2$. The solution mixture was stirred at 300°C until a high viscosity paste was formed. Next the resulting paste was calcined in a crucible alumina pot at 650°C for 2.5 h. Then, 0.04 g of polytetrafluoroethylene (PTFE) powder was added to 1.00 g of $\text{Sn}_{0.9}\text{In}_{0.1}\text{H}_{0.1}\text{P}_2\text{O}_7$ or $\text{Sn}_{0.92}\text{Sb}_{0.08}(\text{OH})_{0.08}\text{P}_2\text{O}_7$ powder, kneaded using a mortar and pestle, and finally cold-rolled to a thickness of $200\ \mu\text{m}$ using a rolling mill. The two membranes obtained in this way were laminated together by pressing at 2 MPa for 2 min. For comparison, $\text{Sn}_{0.9}\text{In}_{0.1}\text{H}_{0.1}\text{P}_2\text{O}_7$ and $\text{Sn}_{0.92}\text{Sb}_{0.08}(\text{OH})_{0.08}\text{P}_2\text{O}_7$ membranes with thicknesses of $400\ \mu\text{m}$ were also prepared.

2.2. Fabrication of Hydrogen/Air Fuel Cell

Commercialized Pt/C electrode ($0.5\ \text{cm}^2$, Electrochem Inc., Woburn, MA, USA) with a Pt loading of $1\ \text{mg}\ \text{cm}^{-2}$ was used for the preparation of the membrane electrode assembly (MEA), and the MEA was fabricated by sandwiching the electrolyte membrane between

the electrodes. Two gas chambers were arranged by placing the MEA between two alumina tubes and sealing the anode side of the MEA with an inorganic adhesive. Unless otherwise stated, unhumidified hydrogen (50 mL min^{-1}) and air (50 mL min^{-1}) saturated by H_2O vapor at room temperature were respectively supplied to the anode and cathode. The fuel cell was operated between 50 and $200 \text{ }^\circ\text{C}$.

2.3. Characterization

The water uptake of the electrolyte membrane was calculated as follows. Prior to water uptake measurements, the fuel cell was operated with a current density of 80 mA cm^{-2} at $100 \text{ }^\circ\text{C}$ for 1 h. Then, part of the electrolyte membrane was immediately removed from the MEA and a thermogravimetric analysis (TGA; Shimadzu, DTG-60, Kyoto, Japan) was conducted from room temperature to $300 \text{ }^\circ\text{C}$ under air with a heating rate of $10 \text{ }^\circ\text{C min}^{-1}$. AC conductivity measurements of the electrolyte membrane were performed under the fuel cell operating conditions. Impedance spectra were collected using an impedance analyzer (Solartron, SI 1260, Farnborough, UK) and an electrochemical interface (Solartron, 1287, Farnborough, UK) in the frequency range from $10\text{--}10^6 \text{ Hz}$ with an AC amplitude of 10 mV. The IR loss of the MEA was determined using the current interruption method. During the measurement, a sharp change in voltage and a slow voltage change indicate IR loss and polarization loss, respectively. A digital oscilloscope (Nicolet, Sigma 75, Gainesville, FL, USA) was used to monitor the change in cell voltage over time.

3. Results and Discussion

The temperature dependency of the electrical conductivity for the $\text{Sn}_{0.9}\text{In}_{0.1}\text{H}_{0.1}\text{P}_2\text{O}_7/\text{Sn}_{0.92}\text{Sb}_{0.08}(\text{OH})_{0.08}\text{P}_2\text{O}_7$ membrane is presented in Figure 2a. For comparison, the conductivities of the individual $\text{Sn}_{0.9}\text{In}_{0.1}\text{H}_{0.1}\text{P}_2\text{O}_7$ and $\text{Sn}_{0.92}\text{Sb}_{0.08}(\text{OH})_{0.08}\text{P}_2\text{O}_7$ membranes were also included. The measurement was conducted under open-circuit conditions at the operating temperatures between 50 and $200 \text{ }^\circ\text{C}$ in air saturated with H_2O vapor at room temperature. The conductivity of these membranes does not follow the Arrhenius-like dependency on temperature, because the RH decreases with increasing temperature (PH_2O rather than RH was maintained constantly at the measurement). However, the electrical conductivity of the heterojunction (i.e., $\text{Sn}_{0.9}\text{In}_{0.1}\text{H}_{0.1}\text{P}_2\text{O}_7/\text{Sn}_{0.92}\text{Sb}_{0.08}(\text{OH})_{0.08}\text{P}_2\text{O}_7$) membrane was comparable to those of the $\text{Sn}_{0.9}\text{In}_{0.1}\text{H}_{0.1}\text{P}_2\text{O}_7$ and $\text{Sn}_{0.92}\text{Sb}_{0.08}(\text{OH})_{0.08}\text{P}_2\text{O}_7$ membranes within the experimental error at all tested temperatures, which implies the absence of an insulating layer at the interface of the heterojunction membrane due to the high compatibility between the $\text{Sn}_{0.9}\text{In}_{0.1}\text{H}_{0.1}\text{P}_2\text{O}_7$ and $\text{Sn}_{0.92}\text{Sb}_{0.08}(\text{OH})_{0.08}\text{P}_2\text{O}_7$ membranes. A similar conclusion has been reported regarding the heterojunction electrolyte composed of proton-conductive yttrium-doped strontium zirconia and oxide ion-conductive yttria-stabilized zirconia [24].

The PH_2O and RH dependency of the electrical conductivity for the $\text{Sn}_{0.9}\text{In}_{0.1}\text{H}_{0.1}\text{P}_2\text{O}_7/\text{Sn}_{0.92}\text{Sb}_{0.08}(\text{OH})_{0.08}\text{P}_2\text{O}_7$ membrane at 50, 100, and $200 \text{ }^\circ\text{C}$ were also evaluated under open-circuit conditions (Figure 2b,c). Although the electrical conductivity increased with increasing PH_2O at all tested temperatures, the PH_2O dependency of the electrical conductivity was the largest at $100 \text{ }^\circ\text{C}$. This result can be interpreted to mean the following: since the membrane is highly hygroscopic at $50 \text{ }^\circ\text{C}$, high electrical conductivity is maintained even under low RH conditions. However, the evaporation of water from the membrane is significant at $200 \text{ }^\circ\text{C}$, thus reducing the humidification effect on the electrical conductivity. These results suggest that the most effective temperature for the self-humidification of the fuel cell is around $100 \text{ }^\circ\text{C}$. Therefore, in subsequent experiments, the fuel cell was operated at $100 \text{ }^\circ\text{C}$.

To observe the water product accumulated in the $\text{Sn}_{0.9}\text{In}_{0.1}\text{H}_{0.1}\text{P}_2\text{O}_7/\text{Sn}_{0.92}\text{Sb}_{0.08}(\text{OH})_{0.08}\text{P}_2\text{O}_7$ membrane during the operation, the membranes were pressed against clean paper before and after operation (Figure 3a,b). Figure 3b clearly shows that the membrane contained a certain quantity of water after the operation that had changed compared to the quantity before the operation. Although care should be taken to account for water

adsorbed on the membrane surface during cell operation, this result indicates that the observed polka-dot trace shown in Figure 3b is mainly attributable to water produced by the self-humidification effect of the membrane. Such traces are substantially less visible when using the individual $\text{Sn}_{0.9}\text{In}_{0.1}\text{H}_{0.1}\text{P}_2\text{O}_7$ and $\text{Sn}_{0.92}\text{Sb}_{0.08}(\text{OH})_{0.08}\text{P}_2\text{O}_7$ membranes as electrolytes.

Further evidence of self-humidification is confirmed by a comparison of TGA profiles for $\text{Sn}_{0.9}\text{In}_{0.1}\text{H}_{0.1}\text{P}_2\text{O}_7/\text{Sn}_{0.92}\text{Sb}_{0.08}(\text{OH})_{0.08}\text{P}_2\text{O}_7$ and the individual $\text{Sn}_{0.9}\text{In}_{0.1}\text{H}_{0.1}\text{P}_2\text{O}_7$ or $\text{Sn}_{0.92}\text{Sb}_{0.08}(\text{OH})_{0.08}\text{P}_2\text{O}_7$ membranes after cell operation. Figure 3c shows that the individual $\text{Sn}_{0.9}\text{In}_{0.1}\text{H}_{0.1}\text{P}_2\text{O}_7$ and $\text{Sn}_{0.92}\text{Sb}_{0.08}(\text{OH})_{0.08}\text{P}_2\text{O}_7$ membranes have similar TGA profiles: A weight loss of ca. 4% occurred in two steps between 50 and 300 °C by the desorption of physically and chemically observed water molecules, respectively [25,26]. Meanwhile the weight loss of the $\text{Sn}_{0.9}\text{In}_{0.1}\text{H}_{0.1}\text{P}_2\text{O}_7/\text{Sn}_{0.92}\text{Sb}_{0.08}(\text{OH})_{0.08}\text{P}_2\text{O}_7$ membrane is approximately two times larger than that observed for the individual $\text{Sn}_{0.9}\text{In}_{0.1}\text{H}_{0.1}\text{P}_2\text{O}_7$ and $\text{Sn}_{0.92}\text{Sb}_{0.08}(\text{OH})_{0.08}\text{P}_2\text{O}_7$ membranes. This result indicates that the increased weight loss is caused by the water produced at the heterojunction, according to Equation (3), then accumulated in the membrane.

If this suggestion is correct, then a decrease in the ohmic resistance or the IR loss of the $\text{Sn}_{0.9}\text{In}_{0.1}\text{H}_{0.1}\text{P}_2\text{O}_7/\text{Sn}_{0.92}\text{Sb}_{0.08}(\text{OH})_{0.08}\text{P}_2\text{O}_7$ membrane would be expected as a result of the operation of the fuel cell because the water produced by self-humidification increases the electrical conductivity. For clarification, electrochemical measurements were conducted. Figure 4 presents the impedance spectra of the fuel cell under open-circuit and DC bias (0.3 V) voltages conditions. The ohmic resistance of the cell with the $\text{Sn}_{0.9}\text{In}_{0.1}\text{H}_{0.1}\text{P}_2\text{O}_7/\text{Sn}_{0.92}\text{Sb}_{0.08}(\text{OH})_{0.08}\text{P}_2\text{O}_7$ membrane was reduced by applying a DC bias voltage (Figure 4a), in contrast to the impedance spectra for the fuel cells with the individual $\text{Sn}_{0.9}\text{In}_{0.1}\text{H}_{0.1}\text{P}_2\text{O}_7$ and $\text{Sn}_{0.92}\text{Sb}_{0.08}(\text{OH})_{0.08}\text{P}_2\text{O}_7$ membranes (Figure 4b,c). The ohmic resistances of the cells with the $\text{Sn}_{0.9}\text{In}_{0.1}\text{H}_{0.1}\text{P}_2\text{O}_7$ and $\text{Sn}_{0.92}\text{Sb}_{0.08}(\text{OH})_{0.08}\text{P}_2\text{O}_7$ membranes remained almost unchanged, despite the fact that polarization of the fuel cells was conducted.

Figure 5a presents the IR losses of the fuel cell over time with a current density of 80 mA cm^{-2} applied to the fuel cells. The IR loss decreased with time until a steady state was reached. The fuel cell with the $\text{Sn}_{0.9}\text{In}_{0.1}\text{H}_{0.1}\text{P}_2\text{O}_7/\text{Sn}_{0.92}\text{Sb}_{0.08}(\text{OH})_{0.08}\text{P}_2\text{O}_7$ membrane shows a decrement in IR loss with time, while those with the individual $\text{Sn}_{0.9}\text{In}_{0.1}\text{H}_{0.1}\text{P}_2\text{O}_7$ and $\text{Sn}_{0.92}\text{Sb}_{0.08}(\text{OH})_{0.08}\text{P}_2\text{O}_7$ membranes are shown to be unchanged during the same period. These results support the self-humidification of the $\text{Sn}_{0.9}\text{In}_{0.1}\text{H}_{0.1}\text{P}_2\text{O}_7/\text{Sn}_{0.92}\text{Sb}_{0.08}(\text{OH})_{0.08}\text{P}_2\text{O}_7$ membrane. In addition, the result of the $\text{Sn}_{0.9}\text{In}_{0.1}\text{H}_{0.1}\text{P}_2\text{O}_7/\text{Sn}_{0.92}\text{Sb}_{0.08}(\text{OH})_{0.08}\text{P}_2\text{O}_7$ membrane also reflects an increase in water uptake with time, and the results imply that it takes approximately 7 min to reach an equilibrium of water uptake into the membrane.

Figure 5b presents the IR loss of the fuel cells as a function of the current density, where data were recorded after steady state was attained. The IR loss of the fuel cell with the $\text{Sn}_{0.9}\text{In}_{0.1}\text{H}_{0.1}\text{P}_2\text{O}_7/\text{Sn}_{0.92}\text{Sb}_{0.08}(\text{OH})_{0.08}\text{P}_2\text{O}_7$ membrane deviated from that estimated (dotted line) from the electrical conductivity at 100 °C, the extent of which increased as the current density increased due to the enhanced self-humidification effect. By contrast, the IR losses of the fuel cells with the individual $\text{Sn}_{0.9}\text{In}_{0.1}\text{H}_{0.1}\text{P}_2\text{O}_7$ and $\text{Sn}_{0.92}\text{Sb}_{0.08}(\text{OH})_{0.08}\text{P}_2\text{O}_7$ membranes almost coincided with the estimated values.

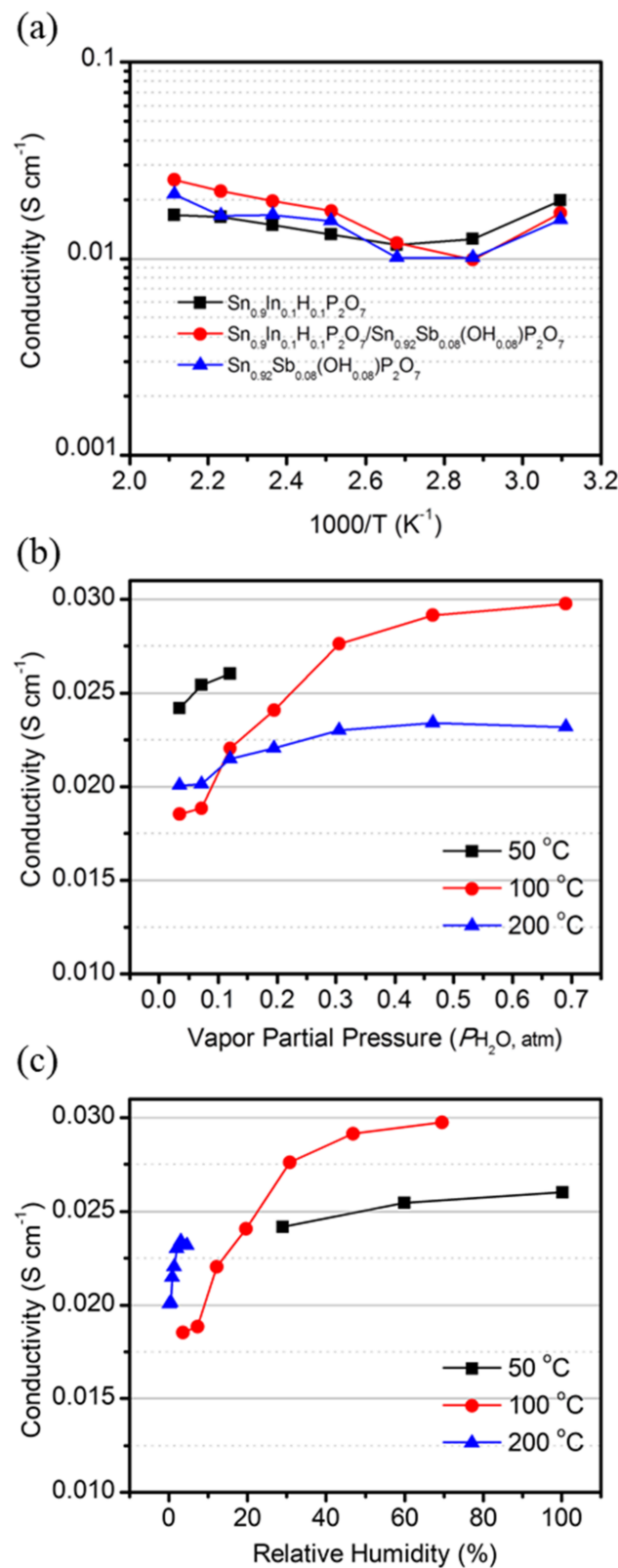


Figure 2. (a) Temperature dependency of electrical conductivity for $Sn_{0.9}In_{0.1}H_{0.1}P_2O_7$, $Sn_{0.92}Sb_{0.08}(OH)_{0.08}P_2O_7$, and $Sn_{0.9}In_{0.1}H_{0.1}P_2O_7/Sn_{0.92}Sb_{0.08}(OH)_{0.08}P_2O_7$ membranes. The measurement was conducted under open-circuit conditions at operating temperatures (50–200 °C) in air saturated with H_2O vapor at room temperature. (b) P_{H_2O} and (c) RH dependency of electrical conductivity for $Sn_{0.9}In_{0.1}H_{0.1}P_2O_7/Sn_{0.92}Sb_{0.08}(OH)_{0.08}P_2O_7$ membrane.

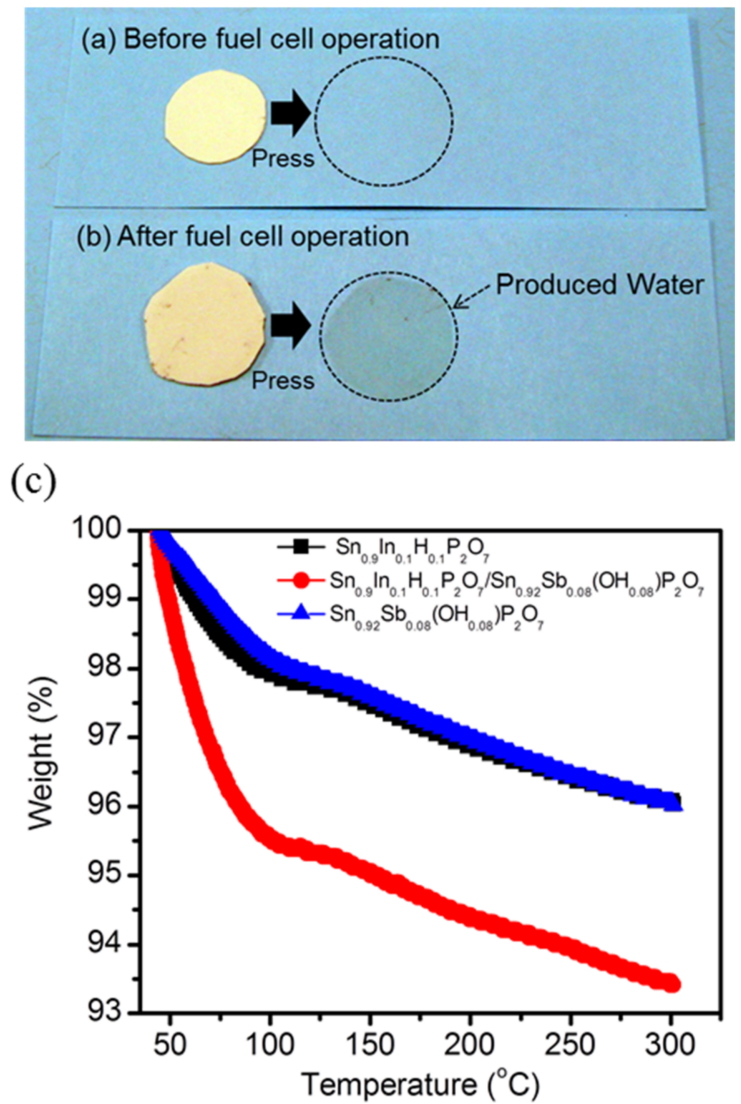


Figure 3. Photo images of water transfer from $\text{Sn}_{0.9}\text{In}_{0.1}\text{H}_{0.1}\text{P}_2\text{O}_7/\text{Sn}_{0.92}\text{Sb}_{0.08}(\text{OH})_{0.08}\text{P}_2\text{O}_7$ membrane to clean paper; (a) before and (b) after fuel cell operation. Dotted circle lines indicate change of clean paper by produced water after pressing the membranes. (c) TGA profiles of membranes.

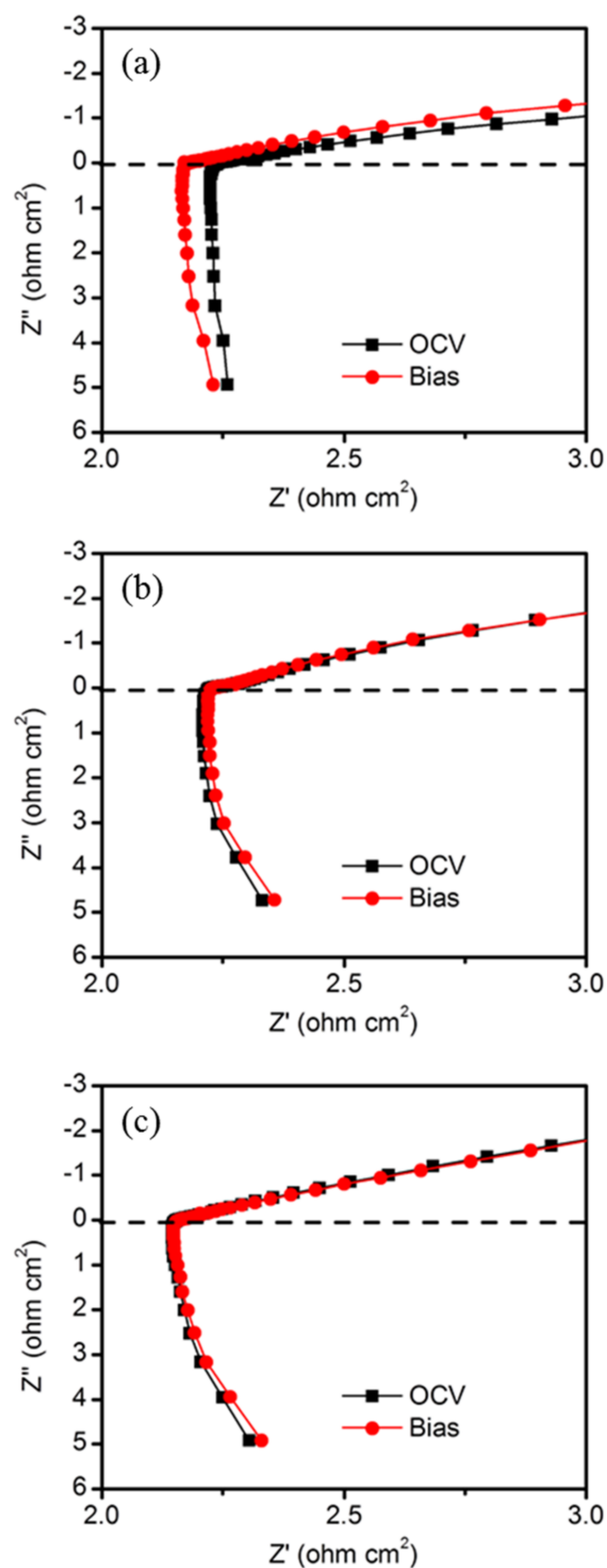


Figure 4. Impedance spectra for (a) $\text{Sn}_{0.9}\text{In}_{0.1}\text{H}_{0.1}\text{P}_2\text{O}_7/\text{Sn}_{0.92}\text{Sb}_{0.08}(\text{OH})_{0.08}\text{P}_2\text{O}_7$ (b) $\text{Sn}_{0.9}\text{In}_{0.1}\text{H}_{0.1}\text{P}_2\text{O}_7$ and (c) $\text{Sn}_{0.92}\text{Sb}_{0.08}(\text{OH})_{0.08}\text{P}_2\text{O}_7$ membranes under open-circuit and DC bias (0.3 V) conditions.

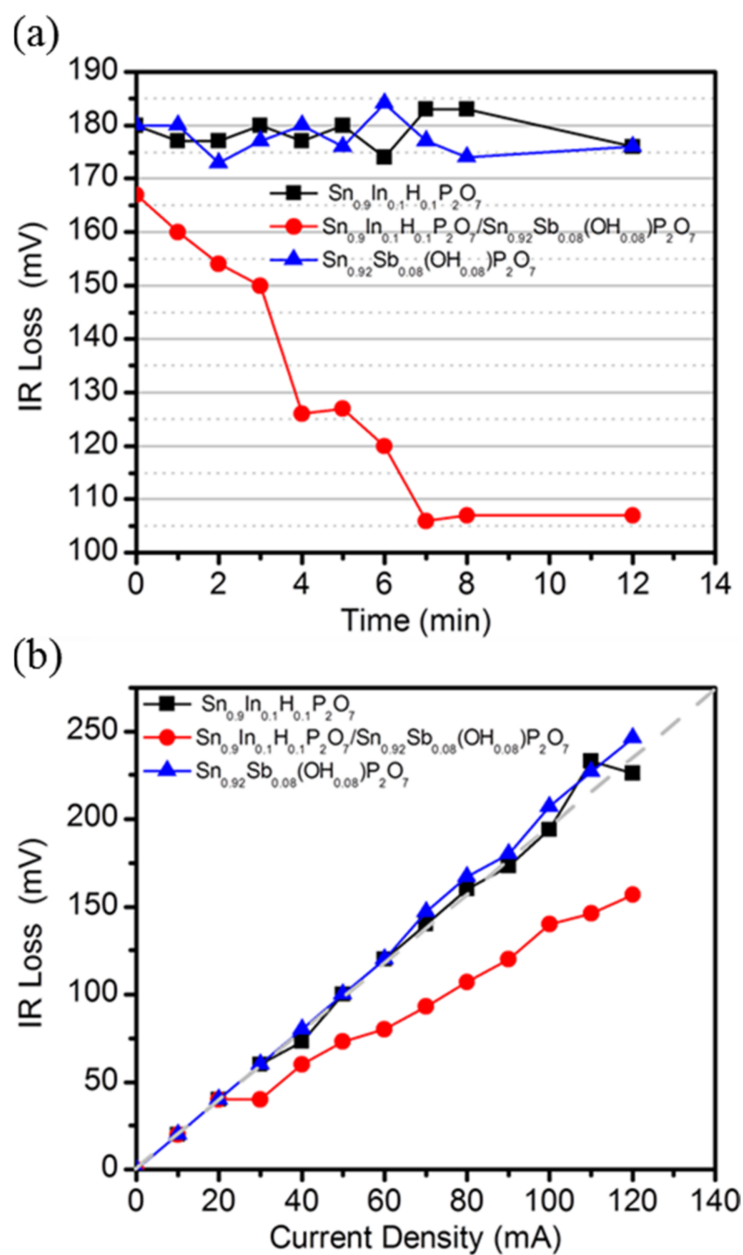


Figure 5. Change in IR losses for $\text{Sn}_{0.9}\text{In}_{0.1}\text{H}_{0.1}\text{P}_2\text{O}_7$, $\text{Sn}_{0.92}\text{Sb}_{0.08}(\text{OH})_{0.08}\text{P}_2\text{O}_7$, and $\text{Sn}_{0.9}\text{In}_{0.1}\text{H}_{0.1}\text{P}_2\text{O}_7/\text{Sn}_{0.92}\text{Sb}_{0.08}(\text{OH})_{0.08}\text{P}_2\text{O}_7$ membranes with respect to (a) time and (b) current density. The cells were operated at 100 °C with unhumidified H_2 and air saturated with H_2O vapor at room temperature ($P_{\text{H}_2\text{O}} = 0.035$ atm) as reactor gases for anode and cathode, respectively.

To clarify the self-humidification effect during the fuel cell performance, the IR losses of the fuel cells with the individual $\text{Sn}_{0.9}\text{In}_{0.1}\text{H}_{0.1}\text{P}_2\text{O}_7$ and $\text{Sn}_{0.92}\text{Sb}_{0.08}(\text{OH})_{0.08}\text{P}_2\text{O}_7$ membranes with different $P_{\text{H}_2\text{O}}$ conditions from 0.035 to 0.690 atm were measured and compared with those of the $\text{Sn}_{0.9}\text{In}_{0.1}\text{H}_{0.1}\text{P}_2\text{O}_7/\text{Sn}_{0.92}\text{Sb}_{0.08}(\text{OH})_{0.08}\text{P}_2\text{O}_7$ membrane at a $P_{\text{H}_2\text{O}}$ of 0.035 atm (Figure 6a,b). A comparison between the fuel cells with the $\text{Sn}_{0.9}\text{In}_{0.1}\text{H}_{0.1}\text{P}_2\text{O}_7/\text{Sn}_{0.92}\text{Sb}_{0.08}(\text{OH})_{0.08}\text{P}_2\text{O}_7$ and individual $\text{Sn}_{0.9}\text{In}_{0.1}\text{H}_{0.1}\text{P}_2\text{O}_7$ or $\text{Sn}_{0.92}\text{Sb}_{0.08}(\text{OH})_{0.08}\text{P}_2\text{O}_7$ membranes confirmed that the IR loss of the former membrane at a $P_{\text{H}_2\text{O}}$ of 0.035 atm was equivalent to that of the latter two membranes at $P_{\text{H}_2\text{O}}$ between 0.465 and 0.690 atm, indicating that the present heterojunction fuel cell can successfully enhance the electrolyte properties without the need for external humidification.

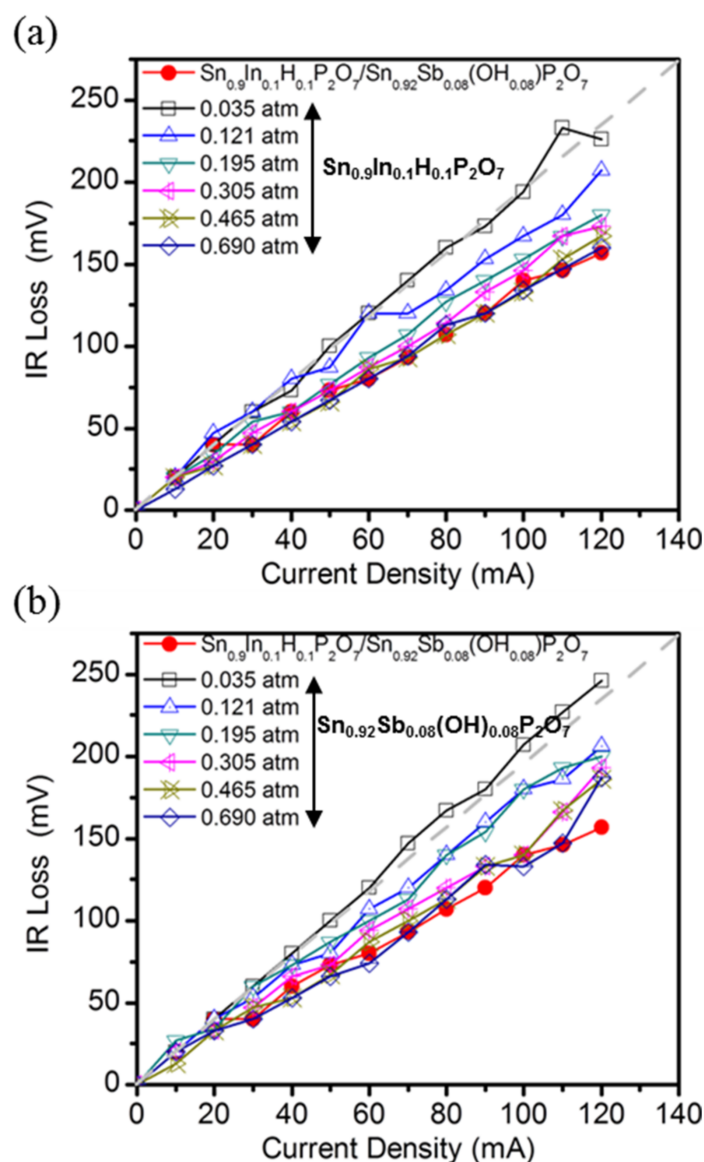


Figure 6. IR losses at different PH_2O conditions of (a) $Sn_{0.9}In_{0.1}H_{0.1}P_2O_7$ and (b) $Sn_{0.92}Sb_{0.08}(OH)_{0.08}P_2O_7$ membranes as a function of current density. Red circle lines indicate IR losses of $Sn_{0.9}In_{0.1}H_{0.1}P_2O_7/Sn_{0.92}Sb_{0.08}(OH)_{0.08}P_2O_7$ membrane at a PH_2O of 0.035 atm.

4. Conclusions

A self-humidifying fuel cell membrane showing the outstanding electrochemical performances at the harsh operating conditions of high temperature and low RH was simply prepared by laminating the proton and anion exchange membranes composed of acceptor-doped SnP_2O_7 composites. The effect of the heterojunction membrane ($Sn_{0.9}In_{0.1}H_{0.1}P_2O_7/Sn_{0.92}Sb_{0.08}(OH)_{0.08}P_2O_7$) on the electrolyte properties was investigated. Since the insulating layer was not formed at the interface between the $Sn_{0.9}In_{0.1}H_{0.1}P_2O_7$ and $Sn_{0.92}Sb_{0.08}(OH)_{0.08}P_2O_7$ membranes, the water absorption of the membrane increased during the fuel cell operation. The comparison of TGA thermograms of the membranes indicated that the water content of the heterojunction membrane was approximately two times larger than the individual $Sn_{0.9}In_{0.1}H_{0.1}P_2O_7$ and $Sn_{0.92}Sb_{0.08}(OH)_{0.08}P_2O_7$ membranes. Therefore, the electrochemical performances of MEAs performance with the heterojunction membrane were substantially better than those with each proton and anion exchange membranes under low RH condition. For example, the IR losses of the heterojunction membrane at current densities of 80 and 120 $mA\ cm^{-2}$ after equilibrium state at 100 °C are 105 and 157 mV, respectively, while those of the $Sn_{0.9}In_{0.1}H_{0.1}P_2O_7$ membrane are 183 and 226 mV,

respectively, and those of the $\text{Sn}_{0.92}\text{Sb}_{0.08}(\text{OH})_{0.08}\text{P}_2\text{O}_7$ membranes are 177 and 246 mV, respectively. Based on the results, we believe that this study can provide insight into the facile preparation of a self-humidifying heterojunction membrane and the wide use of acceptor-doped SnP_2O_7 composites for practical application in high temperature and low RH fuel cells.

Author Contributions: Conceptualization: P.H., K.K.; data curation and investigation: P.H., M.K. and H.K.; formal analysis: P.H., M.K., H.K., S.Y.N., K.K.; funding acquisition: S.Y.N., K.K.; supervision: K.K.; visualization: P.H., M.K., H.K., K.K.; writing—original draft preparation, P.H. and M.K., H.K., S.Y.N., K.K. All authors have read and agreed to the published version of the manuscript.

Funding: This research was supported by the National Research Foundation of Korea funded by the Korean Government (NRF-2019M3E6A1064797, NRF-2019R1F1A1060550, NRF-2020R1A6A1A03038697).

Institutional Review Board Statement: Not applicable.

Informed Consent Statement: Not applicable.

Conflicts of Interest: The authors certify that there is no conflict of interest with any organization regarding the subject matter or materials discussed in the manuscript.

References

1. Peighambardoust, S.J.; Rowshanzamir, S.; Amjadi, M. Review of the proton exchange membranes for fuel cell applications. *Int. J. Hydrog. Energy* **2010**, *35*, 9349–9384. [[CrossRef](#)]
2. Goñi-Urtiaga, A.; Presvytes, D.; Scott, K. Solid acids as electrolyte materials for proton exchange membrane (PEM) electrolysis. *Int. J. Hydrog. Energy* **2012**, *37*, 3358–3372. [[CrossRef](#)]
3. Kim, K.; Heo, P.; Ko, T.; Lee, J.-C. Semi-interpenetrating network electrolyte membranes based on sulfonated poly (arylene ether sulfone) for fuel cells at high temperature and low humidity conditions. *Electrochem. Commun.* **2014**, *48*, 44–48. [[CrossRef](#)]
4. Marcinkoski, J.; Kopasz, J.P.; Benjamin, T.G. Progress in the US DOE fuel cell subprogram efforts in polymer electrolyte fuel cells. *Int. J. Hydrog. Energy* **2008**, *33*, 3894–3902. [[CrossRef](#)]
5. Kim, K.; Choi, S.-W.; Park, J.O.; Kim, S.-K.; Lim, M.-Y.; Kim, K.-H.; Ko, T.; Lee, J.-C. Proton conductive cross-linked benzoxazine-benzimidazole copolymers as novel porous substrates for reinforced pore-filling membranes in fuel cells operating at high temperatures. *J. Membr. Sci.* **2017**, *536*, 76–85.
6. Kim, K.; Heo, P.; Ko, T.; Kim, K.-h.; Kim, S.-K.; Pak, C.; Lee, J.-C. Poly (arylene ether sulfone) based semi-interpenetrating polymer network membranes containing cross-linked poly (vinyl phosphonic acid) chains for fuel cell applications at high temperature and low humidity conditions. *J. Power Sources* **2015**, *293*, 539–547. [[CrossRef](#)]
7. Lee, H.; Han, J.; Ahn, S.M.; Jeong, H.Y.; Kim, J.; Kim, H.; Kim, T.-H.; Kim, K.; Lee, J.-C. Simple and effective cross-linking technology for the preparation of cross-linked membranes composed of highly sulfonated poly (ether ether ketone) and poly (arylene ether sulfone) for fuel cell applications. *J. ACS Appl. Energy Mater.* **2020**, *3*, 10495–10505. [[CrossRef](#)]
8. Han, J.; Lee, H.; Kim, J.; Kim, S.; Kim, H.; Kim, E.; Sung, Y.-E.; Kim, K.; Lee, J.-C. Sulfonated poly (arylene ether sulfone) composite membrane having sulfonated polytriazole grafted graphene oxide for high-performance proton exchange membrane fuel cells. *J. Membr. Sci.* **2020**, *612*, 118428. [[CrossRef](#)]
9. Han, J.; Kim, K.; Kim, J.; Kim, S.; Choi, S.-W.; Lee, H.; Kim, J.-j.; Kim, T.-H.; Sung, Y.-E.; Lee, J.-C. Cross-linked highly sulfonated poly (arylene ether sulfone) membranes prepared by in-situ casting and thiol-ene click reaction for fuel cell application. *J. Membr. Sci.* **2019**, *579*, 70–78. [[CrossRef](#)]
10. Kim, K.; Jung, B.-K.; Ko, T.; Kim, T.-H.; Lee, J.-C. Comb-shaped polysulfones containing sulfonated polytriazole side chains for proton exchange membranes. *J. Membr. Sci.* **2018**, *554*, 232–243. [[CrossRef](#)]
11. Kim, J.; Kim, K.; Ko, T.; Han, J.; Lee, J.-C. Polybenzimidazole composite membranes containing imidazole functionalized graphene oxide showing high proton conductivity and improved physicochemical properties. *Int. J. Hydrog. Energy* **2021**, *46*, 12254–12262. [[CrossRef](#)]
12. Kim, J.H.; Kim, K.; Nam, S.Y. Research Trends of Polybenzimidazole-based Membranes for Hydrogen Purification Applications. *Appl. Chem. Eng.* **2020**, *31*, 453–466.
13. Zelenay, P.; Scharifker, B.; Bockris, J.M.; Gervasio, D. A Comparison of the Properties of $\text{CF}_3\text{SO}_3\text{H}$ and H_3PO_4 in Relation to Fuel Cells. *J. Electrochem. Soc.* **1986**, *133*, 2262. [[CrossRef](#)]
14. Watanabe, M.; Uchida, H.; Seki, Y.; Emori, M.; Stonehart, P. Self-humidifying polymer electrolyte membranes for fuel cells. *J. Electrochem. Soc.* **1996**, *143*, 3847. [[CrossRef](#)]
15. Amjadi, M.; Rowshanzamir, S.; Peighambardoust, S.; Hosseini, M.; Eikani, M. Investigation of physical properties and cell performance of Nafion/TiO₂ nanocomposite membranes for high temperature PEM fuel cells. *Int. J. Hydrog. Energy* **2010**, *35*, 9252–9260. [[CrossRef](#)]

16. Zhang, H.; Zhu, B.; Xu, Y. Composite membranes of sulfonated poly (phthalazinone ether ketone) doped with 12-phosphotungstic acid ($H_3PW_{12}O_{40}$) for proton exchange membranes. *Solid State Ion.* **2006**, *177*, 1123–1128. [[CrossRef](#)]
17. Lee, H.-K.; Kim, J.-I.; Park, J.-H.; Lee, T.-H. A study on self-humidifying PEMFC using Pt–ZrP–Nafion composite membrane. *Electrochim. Acta* **2004**, *50*, 761–768. [[CrossRef](#)]
18. Liang, H.; Dang, D.; Xiong, W.; Song, H.; Liao, S. High-performance self-humidifying membrane electrode assembly prepared by simultaneously adding inorganic and organic hygroscopic materials to the anode catalyst layer. *J. Power Sources* **2013**, *241*, 367–372. [[CrossRef](#)]
19. Liang, H.; Zheng, L.; Liao, S. Self-humidifying membrane electrode assembly prepared by adding PVA as hygroscopic agent in anode catalyst layer. *Int. J. Hydrog. Energy* **2012**, *37*, 12860–12867. [[CrossRef](#)]
20. Su, H.; Xu, L.; Zhu, H.; Wu, Y.; Yang, L.; Liao, S.; Song, H.; Liang, Z.; Birss, V. Self-humidification of a PEM fuel cell using a novel Pt/SiO₂/C anode catalyst. *Int. J. Hydrog. Energy* **2010**, *35*, 7874–7880. [[CrossRef](#)]
21. Heo, P.; Ito, K.; Tomita, A.; Hibino, T. A Proton-Conducting Fuel Cell Operating with Hydrocarbon Fuels. *Angew. Chem.* **2008**, *120*, 7959–7962. [[CrossRef](#)]
22. Jin, Y.; Shen, Y.; Hibino, T. Proton conduction in metal pyrophosphates (MP₂O₇) at intermediate temperatures. *J. Mater. Chem.* **2010**, *20*, 6214–6217. [[CrossRef](#)]
23. Hibino, T.; Shen, Y.; Nishida, M.; Nagao, M. Hydroxide Ion Conducting Antimony (V)-Doped Tin Pyrophosphate Electrolyte for Intermediate-Temperature Alkaline Fuel Cells. *Angew. Chem.* **2012**, *124*, 10944–10948. [[CrossRef](#)]
24. Shimura, T.; Egusa, G.; Iwahara, H.; Katahira, K.; Yamamoto, K. Electrochemical properties of junction between protonic conductor and oxide ion conductor. *Solid State Ion.* **1997**, *97*, 477–482. [[CrossRef](#)]
25. Kim, K.; Kim, S.-K.; Park, J.O.; Choi, S.-W.; Kim, K.-H.; Ko, T.; Pak, C.; Lee, J.-C. Highly reinforced pore-filling membranes based on sulfonated poly (arylene ether sulfone) s for high-temperature/low-humidity polymer electrolyte membrane fuel cells. *J. Membr. Sci.* **2017**, *537*, 11–21. [[CrossRef](#)]
26. Hickner, M.A.; Ghassemi, H.; Kim, Y.S.; Einsla, B.R.; McGrath, J.E. Alternative polymer systems for proton exchange membranes (PEMs). *Chem. Rev.* **2004**, *104*, 4587–4612. [[CrossRef](#)]